

**Serpulids as indicators of mid-late Holocene climate:
Timing and paleoclimate significance of large worm tube aggregates,
Lago Enriquillo, Dominican Republic.**

SENIOR THESIS

Whitney C. Doss
Advisor: Lisa Greer

Submitted in partial fulfillment of Bachelor of Science Degree with Honors in Geology

Washington & Lee University
2006

TABLE OF CONTENTS

The contents of this paper were presented as a talk at the annual Keck Research Symposium in Geology at Amherst College in April 2006, and as posters at the Annual Geologic Society of America Conference in Salt Lake City, Utah in October 2005, the National Conference for Undergraduate Research at Virginia Military Institute in April 2005, and the R.E. Lee Summer Research poster session, Washington & Lee University in October 2004.

Abstracts have been published in 2005 GSA Abstracts with Programs and the Nineteenth Annual Keck Research Symposium in Geology Proceedings, 2006.

Serpulid Worm Tube Mounds	
Serpulid Worms	
Stable Isotope Theory	
Methods.....	9
Site Characterization and Sample Collection	
Sample Preparation	
High Resolution Sampling	
Stable Isotope Analysis	
Uranium/Thorium Age Dating	
Radiocarbon Age Dating	
Results.....	14
Field Mapping and Observations	
Geochemical Data	
Bulk Stable Carbon and Oxygen Isotope Data	
High Resolution Stable Carbon and Oxygen Isotope Data	
Age Dating	
Discussion.....	22
Conclusion.....	25
Acknowledgements.....	27
References.....	28
Appendix A.....	29
High Resolution Stable Isotope Data	
Appendix B.....	33
Bulk Stable Isotope Data	

TABLE OF CONTENTS

Abstract.....	1
Introduction.....	2
Background.....	3
Regional Setting	
Serpulid Worm Tube Mounds	
Serpulid Worms	
Stable Isotope Theory	
Methods.....	9
Site Characterization and Sample Collection	
Sample Preparation	
High Resolution Sampling	
Stable Isotope Analysis	
Uranium/Thorium Age Dating	
Radiocarbon Age Dating	
Results.....	14
Field Mapping and Observations	
Geochemical Data	
Bulk Stable Carbon and Oxygen Isotope Data	
High Resolution Stable Carbon and Oxygen Isotope Data	
Age Dating	
Discussion.....	22
Conclusion.....	25
Acknowledgements.....	27
References.....	28
Appendix A.....	29
High Resolution Stable Isotope Data	
Appendix B.....	33
Bulk Stable Isotope Data	

ABSTRACT

Large aggregates of calcareous serpulid worm tubes recorded paleoclimate conditions as they colonized the mid to late Holocene Enriquillo embayment, Dominican Republic. Serpulid worms flourished in the embayment following the demise of a coral reef complex due to the abrupt cessation of normal marine circulation. While serpulid tubes are found in thin layers and as single tubes encrusting corals in normal marine deposits around the present-day hypersaline lake, they dominated the initial restricted environment in a unique aggregate form. Large monospecific mounds up to 2.8 m in height cap the reef sequence and occur in tiers marking the extent of different paleoshorelines around the periphery of the valley. Initially, serpulids colonized hard coral substrates such as large *Montastraea annularis* colonies and *Acropora cervicornis* rubble, but some may have even colonized live coral. The mounds are coated with a thick tufa rind. Stable carbon and oxygen isotopic data in conjunction with $^{230}\text{Th}/^{234}\text{U}$ and C-14 dating suggest a transition to hyposaline conditions ~4000 ybp, about the time of the earliest mound accumulation. High resolution geochemical analyses indicate that sub-annual paleoenvironmental data may be extracted from individual serpulid tubes. Results of high resolution sampling from individual tubes indicate considerable variability in temperature and salinity conditions throughout the period of tufa-coated serpulid mound formation, significantly more so than in tubes formed under normal marine conditions. Also, data suggests that an overall Holocene transition from warm/wet to more arid climate patterns resulted in the closure of the embayment and the creation of optimal conditions for such massive serpulid colonies.

INTRODUCTION

Many species of coral, foraminifera, and ostracods are frequently used as proxies for environmental conditions. This paper applies the same theory and methodology to serpulid worm tubes. Not only may slight seasonal variations in climate be studied through high resolution sampling of single tubes, but larger-scale changes over many hundreds of years may be understood through the interpretation of overall mound morphology and geochemical composition. Here geochemistry is used as a tool to understand the physical formation of these mounds to gain insight into the environmental changes the area underwent during this time period.

As alluvial shedding from the mountains began to stifle the marine transgression in the Enriquillo Valley, the bay transitioned to an ephemeral, hyposaline environment. The uniquely large serpulid tube aggregates represent not just an ecological succession, but a dynamic shift in regional climate from warm/wet to more arid conditions. Stable carbon and oxygen isotopic compositions and age data enable serpulid tubes to relate (1) the type of setting in which the tube formed in terms of normal marine versus hyposaline conditions (2) the variability of the environment in which a single tube or a whole mound grew (3) individual storm events or a period of storm intensification (4) the onset and termination of mounds as signals of greater-scale climate change. This study attempts to place Enriquillo Valley's paleoclimate history into a regional or larger-scale context.

BACKGROUND

Regional Setting

Lago Enriquillo is located in southwestern Dominican Republic. This country occupies the eastern half of the Caribbean island of Hispaniola and adjoins Haiti to the west. The fault-bounded Enriquillo/Cul-de-Sac Valley trends east-west across southern Hispaniola (Figure 1) and extends 130 km from the Bahia de Neiba in the Dominican Republic to the Baie de Port-au-Prince in Haiti (Mann et al., 1984). All 265 km² of Lago Enriquillo is situated within the Dominican Republic, and it occupies the area known as the Enriquillo Valley (Figure 1).

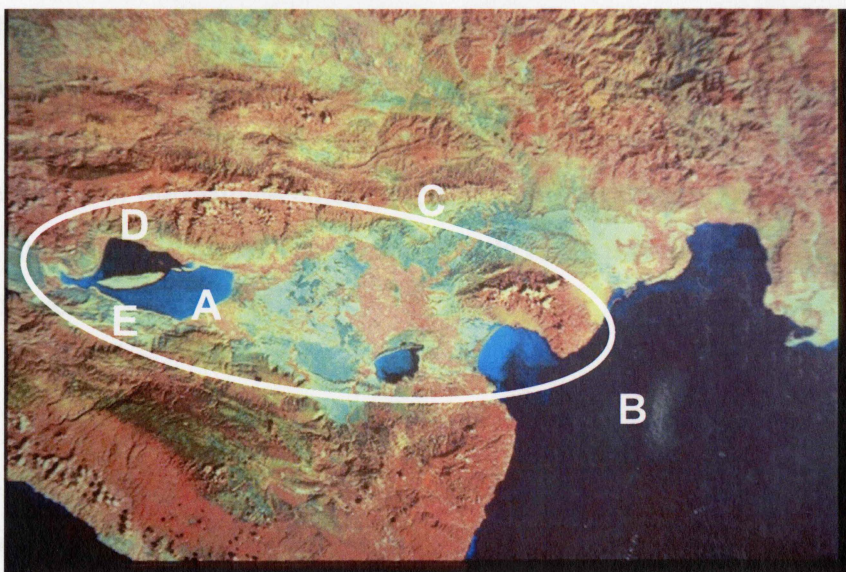


Figure 1. Aerial view of the Enriquillo Valley. (A) Lago Enriquillo (B) Bahia de Neiba (C) Location of paleo-seaway, cut off during the mid-Holocene (D) Approximate location of study site Cañada Honda (E) Approximate location of study site Abuela Grande.

Following the last ice age, sea level rise flooded the valley creating an 85 km long by 12 km wide embayment (Mann et al., 1984). In response to the subsequent rise in base level erosion or other climate-driven factors such as precipitation increase, sediments were shed from the surrounding mountains and dumped in the mouth of the embayment (Taylor et al., 1985). This damming effect in combination with possible vertical fault scarp movement effectively ended circulation with the Caribbean Sea. Evaporation resulted in the present-day hypersaline Lago Enriquillo ~40 m below sea

level. Presently, only ~60 cm of rainfall is received annually, maintaining lake salinity at 60-90 ppt (Schubert, 2000). The main channel of the Enriquillo watershed, the Rio Yaque del Sur, has periodically been diverted into Lago Enriquillo although it is currently draining into the Caribbean Sea (Greer and Swart, in press).

After the valley ceased to be an arm of the sea and water level subsided, thick sequences of coral reef and related carbonate strata deposited in the full marine setting were exposed. The semiarid climate provided an ideal setting in which to preserve the aragonite and calcite deposits (Figure



Figure 2. Excellently preserved, in situ coral reef complex from Lago Enriquillo

2). The Holocene reef has experienced little recrystallization or cementation, and three-dimensional outcrops exposed in arroyos reveal the reef in the same orientation as it grew underwater (Figure 2). Proof of the extraordinarily pristine condition of fossils is found in the preservation of the original color of some mollusk species, many of which are still articulated. In addition, Jackson (2005) found little to no alteration of corals from aragonite to calcite.

Serpulid Worm Tube Mounds

The coral reef sequence, exposed subaerially, is located approximately 3 to 30 meters below present sealevel (Guerard et al., 2004) and capped by large aggregates of



Figure 3. Contact of serpulid tube mound on platy *Montastraea Annularis* at Abuela Grande, Lago Enriquillo.

serpulid worm tubes. In fact, the most predominant, consistent contact in the area is mound on substrate (Figure 3). The substrate character is other mounds or well-indurated *Acropora cervicornis* rubble. However, some mounds appear to have colonized on live *A. cervicornis* or even *Montastrea annularis* in places (Figure 3).

Mounds accumulated in a variety of shapes and sizes. Generally formless, low-relief, <1 m mounds dot the landscape in flat-

lying fields (Figure 4a), while large >3 m mounds are laterally extensive as two consecutive tiers on steep cliff faces (Figure 4b). The largest mounds occur at the highest elevation and appear as if “smeared” in a straight horizon across the Miocene limestone of the mountainside. Large, hemispherical ~ 2.8 m tiered mounds are also found on gentler slopes (Figure 4a) and like the cliff mounds form planar terraces. Closer to the lake shore on little to no slope are laterally extensive mound fields. Here, these mounds typically reach dimensions no larger than 1 m (Figure 4c).

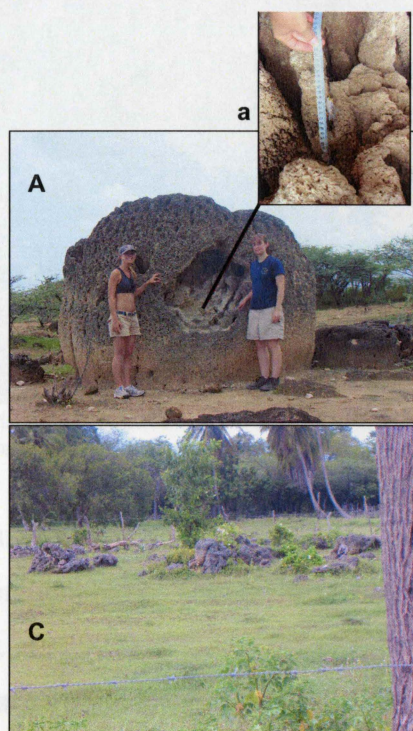
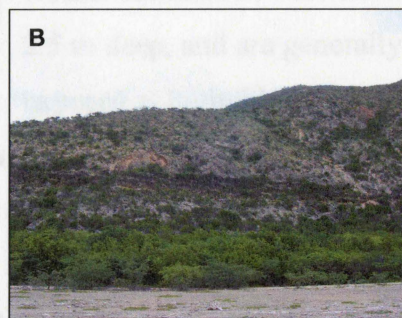


Figure 4. Examples of three variations of serpulid mound morphology. The top of a large capping mound (A) has caved in, exposing the columnar inner structures (a). Terraced cliff-mounds on a steep, northern shore cliff face (B). Irregularly spaced aggregates in a lakeside pasture lack a distinct form (C).



All mounds display weathered outer surfaces. Most mounds exhibit a characteristic “organ-pipe” structure (Glumac et al., 2004) with columnar heads merging at the top of the mound (Figure 4). In addition to a weathered, tufa-coated outer surface, many mounds are also extensively bored and encrusted with *Chama* sp. clams.

A thick tufa rind coats the exterior of mounds at most locales around the lake. This well-indurated outer layer is comprised of mainly low-magnesium calcite (Mann et al, 1984; Glumac et al., 2004). Previously taken photomicrographs show a porous, micritic, microsparitic, and peloidal carbonate cement surrounding the elliptical serpulid

tubes (Glumac et al., 2004). Similarity between the composition of the serpulid tubes and the tufa may suggest contemporaneous deposition (Glumac et al, 2004).

Serpulid Worms

Serpulids are sessile, polychaete annelids which protrude out of their tubes in order to filter feed. Present-day serpulid species exist in mound form but rarely do accumulations attain the size of those at Lago Enriquillo. Observation of modern

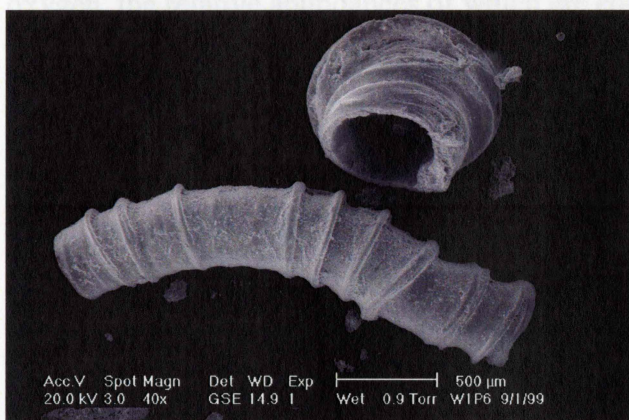


Figure 5. S.E.M. photo of serpulid worm tube showing bell-shaped accretion structures that may indicate seasonal growth.

serpulid reefs in Baffin Bay suggests serpulids are a euryhaline animal, able to withstand variable environmental conditions (Glumac et al, 2004).

Tubes can grow to ~2 cm in length, and form bell-shaped accretion ridges (Figure 5). These filter-feeding worms colonize in waters from 0.5 to 2.5 m deep, and are generally not exposed at high tide (Andrews, 1964).

Previous studies indicate that serpulids secrete calcite tubes with $\delta^{18}\text{O}$ in equilibrium with their environment but $\delta^{13}\text{C}$ may deviate by about -7 to -4 per mil due to vital effects (Glumac et al., 2004).

Most serpulid species traditionally have been considered secondary frame builders, meaning they fill and cement open spaces in a coral reef or other submerged substrate. However, many recent serpulid species are now thought to be primary frame builders – pioneer organisms which accrete the main structure of a reef, and whose biomass accounts for the majority of reef buildup (Hove and van den Hurk, 1993). Although the exact species name of the Lago Enriquillo fossil serpulids is presently unknown, they exhibit similar characteristics to other primary frame building serpulid species found in both the fossil record and in present-day live colonies. Modern examples include *Serpula vermicularis* reefs in Ardbear Lough, Ireland, and aggregates in Baffin Bay, Texas thought to be *Hydroides dianthus* (Hove and van den Hurk, 1993).

Stable Isotope Theory

Stable isotope theory suggests that serpulid tubes may serve as proxies for environmental conditions. As the serpulid worm grows, it incorporates carbon and oxygen from the surrounding water into its calcite tube. Each tube segment, powdered, dissolved and run through a stable isotope mass spectrometer, essentially provides a "snapshot" of the stable isotopic condition of the water in which the mineral was precipitated. There are several naturally occurring stable isotopes for both carbon and oxygen, the relative abundances of which are controlled by a variety of different mechanisms. By determining the ratio of $^{13}\text{C}/^{12}\text{C}$ and $^{18}\text{O}/^{16}\text{O}$ of consecutive tube segments and whole tubes, we may note changes taking place in the ratio values and consequently interpret changes in surrounding environmental conditions. Ratios can be represented as $\delta^{13}\text{C}$ and $\delta^{18}\text{O}$.

In order for high resolution sampling to provide more than just a range of $\delta^{13}\text{C}$ and $\delta^{18}\text{O}$ values and general variability trends, the growth rate of serpulid tubes must be identified. The timescale represented is dependent upon tube growth rates. Growth rates of presumably closely related modern serpulids can be considered. Hove and van der Hurk (1993) estimate a growth rate of 1-4 mm per month, depending on environmental conditions. Bosence (1979) determined a higher growth rate of 9 mm in length over a one month period. Behrens (1968) gave a more complex formula of 1.5-2.5 mm/day for the first three days, followed by a decrease in rate of 0.8-1.3 mm/day for the next two to four weeks. After this, the rate decreases further to 0.1-0.2 mm/day. If the Behrens calculations are accurate, a maximum measured length of an individual tube of ~3 cm could represent between 150-300 days growth. It may thus be assumed that the differences in isotopic composition of segments of individual tubes reflect variations on an annual/seasonal scale.

Stable oxygen isotopes reflect the temperature of the surrounding water due to kinetic effects, or the oxygen isotope composition of the water as controlled by evaporation/precipitation. The latter effect basically represents the relative salinity of the water. The lighter the stable oxygen ratio ($\delta^{18}\text{O}$) the warmer and/or the less saline the water. It is oftentimes difficult to distinguish between the two effects; that is, to understand which force is responsible for an observed change in isotopic ratio values.

METHODS The flux of organic matter into a system may be investigated by use of stable carbon isotopes. Although drawing conclusions from stable carbon isotopes is not as well understood, it is known that terrestrially derived carbon has an isotopically lighter signature than does marine carbon. Thus, the source of organic carbon in the water may be explored through stable carbon isotopes. Relatively lighter ratios ($\delta^{13}\text{C}$) may signify more input of terrestrial carbon material into the body of water.

The study site was surveyed at Canada Heads by documenting elevation and location with a GPS handheld unit and a Jacob's staff. Geographic (GPS) coordinates are given using WGS 1984 earth fixed global reference frame. Mounds were then categorized according to elevation and morphology. Aggregates found closest to the lake were termed island mounds due to their sporadic, isolated arrangement. Further uplope, from lowest to highest elevation, are located terraces 1a, 2a, 3a, and 4a, with laterally continuous substrate contacts termed 1, 2, 3, and 4 (Figure 6).

A laterally continuous 58.5 m long profile was identified from a low elevation island mound to a capping tier 4a along the valley slope. GPS coordinates were obtained at all mound terraces and contacts. Samples were collected at both the sporadic mounds and coral substrates, and sampling sites were marked on the profile. Tubes were removed from both aggregate samples as well as from pieces of coral collected at stratigraphic contacts between mounds.

A high resolution sampling of vertical transect tubes was performed from the base of tier 3a to the top of tier 4a (Figure 7). Small sections of aggregated tubes were extracted in 5-10 cm intervals, with some discontinuities due to slumping, erosion, or thick tuff coating - in these cases the sampling line was shifted laterally in order to avoid collecting transported tubes. The tier 3a transect was selected for its freshly exposed surfaces along a road cut (Figure 7). The 4a transect is located slightly west of the selected 3a mound, and was sampled along fresh surfaces exposed by a recent vertical uplift in the mound.

FIGURE 6. (following page)

Schematic diagram showing relative locations of each tier and contact at the Canada Heads study site. GPS coordinates for the origin and base of the profile are given. Photos give examples of mounds found at each terrace.

METHODS

Site Characterization and Sample Collection

Mound characterization used throughout this paper was developed primarily from field observations at the Canada Honda ($18^{\circ}32.030''$ N, $71^{\circ}37.202''$ W) and Abuela Grande ($18^{\circ}24.462''$ N, $71^{\circ}36.707''$ W) locales. Serpulid mounds were surveyed at Cañada Honda by documenting elevation and location with a GPS handheld unit and a Jacob's staff. Geographic (GPS) coordinates are given using WGS 1984 earth fixed global reference frame. Mounds were then categorized according to elevation and morphology. Aggregates found closest to the lake were termed island mounds due to their sporadic, isolated arrangement. Further upslope, from lowest to highest elevation, are located terraces 1a, 2a, 3a, and 4a, with intermittent substrate contacts termed 1, 2, 3, and 4 (Figure 6).

A laterally continuous 58.5 m long profile was identified from a low elevation island mound to a capping tier 4a along the valley slope. GPS coordinates were obtained at all mound terraces and contacts. Samples were collected at both the serpulid mounds and coral substrates, and sampling sites were marked on the profile. Tubes were removed from both aggregate samples as well as from pieces of coral collected at stratigraphic contacts between mounds.

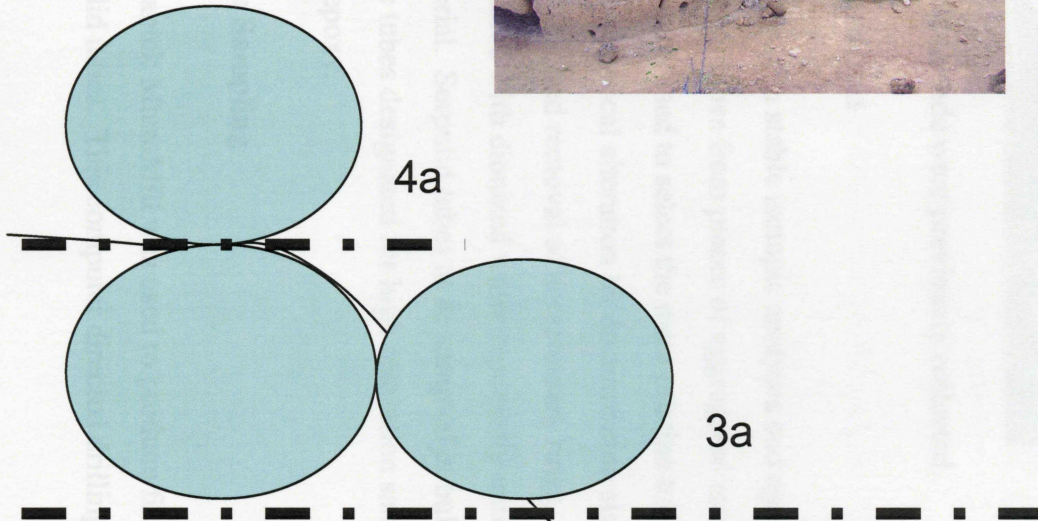
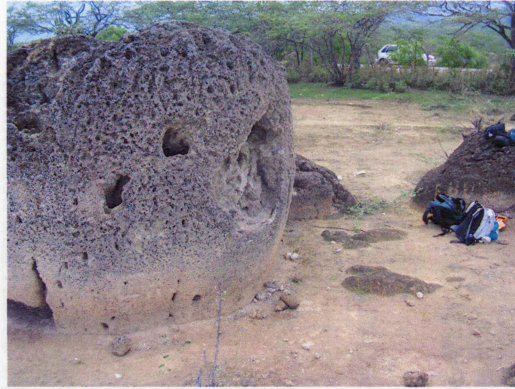
A high resolution sampling of serpulid worm tubes was performed from the base of tier 3a to the top of tier 4a (Figure 7). Small portions of aggregated tubes were extracted at 5-10 cm intervals, with some discontinuance due to slumping, erosion, or thick tufa coating – in these cases the sampling line was shifted laterally in order to avoid collecting transported tubes. The tier 3a transect was selected for its freshly exposed surfaces along a road cut (Figure 7). The 4a transect is located slightly west of the selected 3a mound, and was sampled along fresh surfaces exposed by a recent vertical split in the mound.

FIGURE 6. (following page)

Schematic diagram showing relative locations of each tier and contact at the Canada Honda study site. GPS coordinates for the origin and base of the profile are given. Photos give examples of mounds found at each terrace.

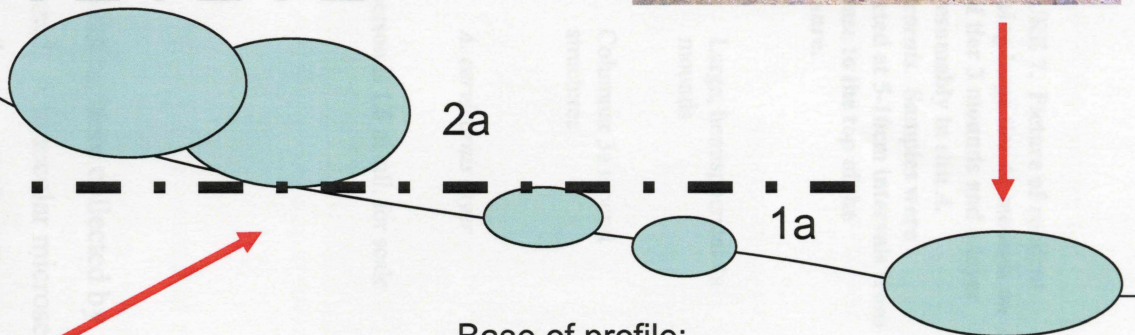


Origin of profile:
18°32'1.24"N,
71°37'9.53"W



Explanation

- mound
- tier contact
- current topography
- A. cervicornis* layer



Base of profile:
18°31'59.55"N,
71°37'10.12"W

Island mound

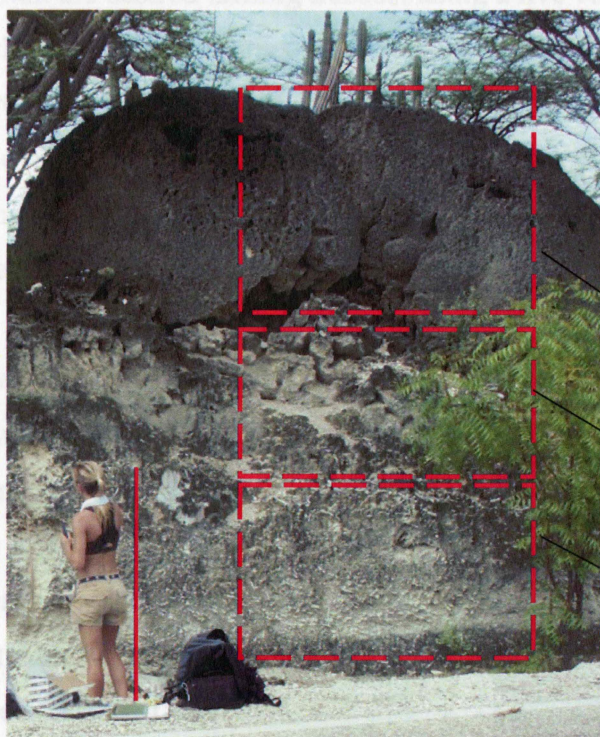


FIGURE 7. Picture of roadcut exposing large tier 4a mounds on top of tier 3 mounds and a layer of presumably in situ *A. cervicornis*. Samples were collected at 5-10cm intervals from the base to the top of the exposure.

Large, hemispherical 4a mounds

Columnar 3a mound structures

A. cervicornis layer

*person is 1.6 m tall, for scale

Samples at Abuela Grande were previously collected.

Sample Preparation

Samples for both stable isotopic analyses and age dating were collected by extracting individual tubes from pieces of aggregated mound. A binocular microscope and dental picks were used to select the most pristine tubes for sampling. All samples were assessed for chemical alteration by documenting signs of weathering, including discoloration, cracks, and removal of accretionary rings. Tubes were cleaned by sonication and rinsed with dionized water repeatedly until decanted water was clear of any detrital material. Serpulid tubes to be sampled in bulk were crushed with a mortar and pestle, while tubes designated for high resolution sampling were attached to a clean glass slide with epoxy.

High Resolution Sampling

A Merchantek MicroMill was used to produce finely powdered carbonate from individual serpulid tubes. This computer directed drilling device allows the operator to

program the desired drilling transect using a live video feed of the sample stage, and then watch on a computer screen as the drill automatically performs the scan (Figure 8). The MicroMill enabled a small amount of powder to be removed from consecutive segments of the tube, resulting in high resolution data which reflects the environmental changes during the life span of a single organism. Whole tubes powdered in bulk yield only the average conditions at the time of tube growth.

The number of samples per tube ranged from 3 to 18, with 6 being the average number of samples per tube. Segments were drilled until sufficient ($\sim 50 \mu\text{g}$) amounts of powder were generated, with no standard segment length due to natural variations in the shape and size of each tube.

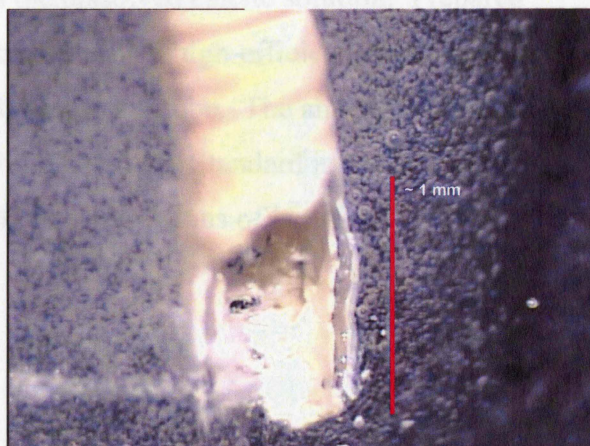


Figure 8. MicroMill drill-view photo of partially drilled tube.

Stable Isotope Analysis

At the University of Saskatchewan, the powdered samples were roasted in a vacuum oven at 200°C for 1 hour in order to completely remove water and any other volatile contaminants. Stable isotope values were obtained using a Finnigan Kiel-III carbonate preparation device directly coupled to the dual inlet of a Finnigan MAT 253 isotope ratio mass spectrometer. Stable isotope values at Lamont-Doherty Earth Observatory were measured on a MICROMASS Optima Mass Spectrometer equipped with a multiprep sample introduction device.

Isotopic ratios were corrected for acid fractionization and ^{17}O contribution, and are reported in permil notation ($^{\circ}/_{\text{oo}}$) relative to the Vienna PeeDee Belemnite standard (VPDB). Precision and calibration were monitored by regular use of a laboratory standard, and standard deviations for $\delta^{13}\text{C}$ and $\delta^{18}\text{O}$ are 0.05‰ and 0.10‰ , respectively (one sigma).

Uranium/Thorium Age Dating

$^{230}\text{Th}/^{238}\text{U}$ age dates were obtained using Multi-Collector Magnetic Sector Inductively Coupled Plasma Mass Spectrometry at Lamont-Doherty Earth Observatory. Prior to analysis by the PLASMA 54, the serpulid worm tubes selected for age dating were processed through standard anion exchange column chemistry in order to separate Uranium, Thorium, and Protactinium from the dissolved calcite solution. Prepared samples were introduced to the mass spectrometer by a high-efficiency nebulizer, permitting the testing of fragments as small as a worm tube. The analytical precision is typically better than +/- .3% for $^{230}\text{Th}/^{238}\text{U}$ (two sigma). Standard isotope dilution equations are employed to back calculate the concentrations of Uranium and Thorium in each sample (Mortlock et. al., 2005).

Radiocarbon Age Dating

Radiocarbon age dates were obtained using a 10 MV Tandem Van de Graaff Accelerator at Lawrence Livermore National Laboratory. The quoted age is in radiocarbon years using the Libby half life of 5568 years. The dates were calibrated into calendar years using CALIB Radiocarbon Calibration 5.0.2.html. Uncertainty is within 0.5 to 1% (one sigma) corresponding to +/- 40 years in a radiocarbon date.

TIER	N (18 deg)	W (71 deg)	HAE (m)
4a	32°01.24"	37°03.53"	-23.48
3a	31°59.95"	37°09.74"	-30.3
2a	31°59.34"	37°10.08"	-33.0
2a	31°59.42"	37°09.89"	-34.3
Island	31°59.99"	37°11.55"	-37.40
Island	31°54.56"	37°16.72"	-44.17

While the cemented serpulid aggregates are predominantly monospecific, other fossilized organisms are dispersed throughout mixed formations. Mussel beds, gastropod shells, encrusting clam species, and lithophilic trace fossils are present along the sides and bases of mounds. Less profuse yet by no means scarce are coral encrusters such as *Millepora* sp. attached to the *A. cervicornis* rubble and bases of mounds.

RESULTS

Field Mapping and Observations

Mound morphology varies with elevation and location. Mounds closest to the present-day lake shore are isolated “island” mounds colonizing massive *Montastraea annularis* coral colonies. These single-tiered structures are low relief, lobate serpulid aggregates ringing the coral accumulations (Figure 6) with more developed growth on the leeward side. Four levels of laterally extensive mound terraces on a steeper gradient exist upslope from the sporadic island mounds: tiers 1a, 2a, 3a, and 4a. Unlike the somewhat amorphous mounds of the lowest elevations, the terraced mounds have a hemispherical shape with a distinctive organ-pipe structure (Figure 6). The lowest level consists of small, squat, “muffin” shaped formations (Figure 6). The second tier displays larger more closely spaced mounds that colonized *A. cervicornis* rubble. This coral pavement is well indurated. Pieces of packed coral also serve as substratum for the third tier, though a recent road cut reveals a cross-section of fairly pristine *A. cervicornis* directly underneath third tier mounds. The third and fourth tiers contain the largest mounds, with a maximum measured circumference of 12.9 m and height of 2.9 m. The uppermost mounds sit directly atop the third terrace (Figure 6). Two coalesced mound tiers rim the paleoshorline along the rocky northern cliffs of the valley (Figure 4c).

TIER	N (18 deg)	W (71 deg)	HAE (m)
4a	32°01.24"	37°09.53"	-26.48
3a	31°59.95"	37°09.74"	-30.8
2a	31°59.34"	37°10.06"	-33.0
2a	31°59.42"	37°09.89"	-34.2
Island	31°59.99"	37°11.55"	-37.48
Island	31°54.56"	37°16.72"	-44.17

Table 1 (at left). GPS coordinates of randomly selected serpulid mounds from tiers 4a, 3a, 2a, and “island” locales. These coordinates are all located along the sampling profile. HAE stands for “height above ellipsoid.”

While the cemented serpulid aggregates are predominantly monospecific, other fossilized organisms are dispersed throughout mound formations. Mussel beds, gastropod shells, encrusting clam species, and lithophagid trace fossils are present along the sides and bases of mounds. Less profuse yet by no means scarce are coral encrusters such as *Millepora sp.* attached to the *A. cervicornis* rubble and bases of mounds.

Serpulid tubes are also found in thin layers and as single tubes encrusting corals in normal marine deposits around the lake. At Abuela Grande, there is a thin yet stratigraphically distinct serpulid layer which overlies in situ reef deposits and underlies the full-fledged mounds (Guerard et. al., 2004). This low-diversity assemblage is markedly separate from the normal marine facies. Serpulid tubes found amongst seemingly healthy coral at Cañada Honda and Abuela Grande sites do not occur in such layered aggregates and colonized substrates individually instead.

Geochemical Data

Bulk Stable Carbon and Oxygen Isotope Data

The average stable carbon and oxygen isotope values of tubes from three distinct sample populations (normal marine tubes, tubes from the low diversity layered deposits, and mound tubes) are distinctly different. (Figures 10 and 10a).

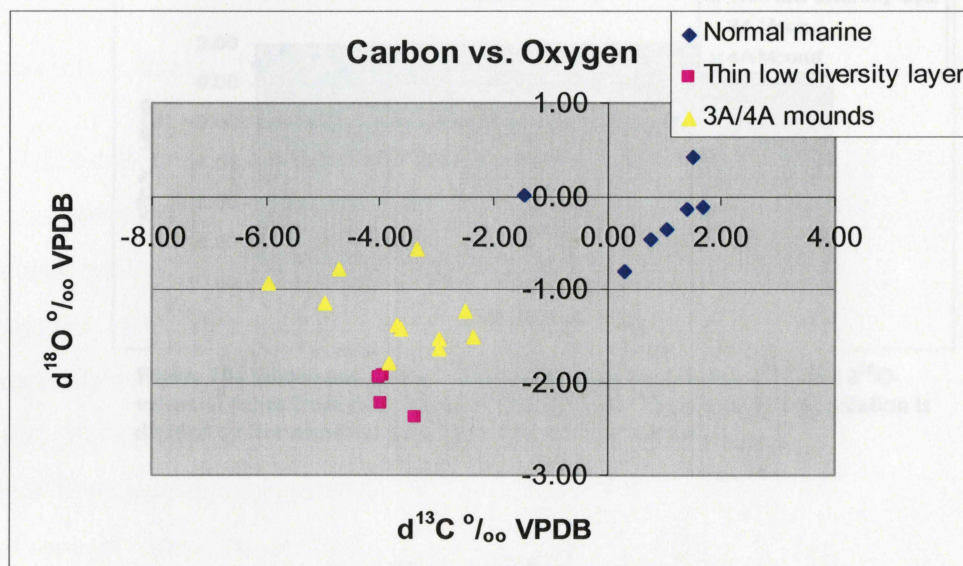


Figure 10. Plot of $\delta^{18}\text{O}$ versus $\delta^{13}\text{C}$ for three sample populations. Each data point represents the average composition for one whole tube analyzed – i.e. “bulk data”.

Samples collected from the normal marine setting display the highest $\delta^{13}\text{C}$ and $\delta^{18}\text{O}$ (1.67 ‰ VPDB and 0.41 ‰ VPDB, respectively). Tubes taken from the short-lived thin diversity layer show little variation in both $\delta^{13}\text{C}$ (0.58 ‰ VPDB) and $\delta^{18}\text{O}$ (0.44 ‰ VPDB). Mound tubes display the largest amount of variation in both $\delta^{13}\text{C}$ and $\delta^{18}\text{O}$ (3.61 ‰ VPDB and 1.23 ‰ VPDB, respectively). Although the average $\delta^{13}\text{C}$ for

mound tubes and thin layer tubes is roughly the same (-3.85 ‰ VPDB $\delta^{13}\text{C}$ and -3.82 ‰ VPDB $\delta^{18}\text{O}$), the $\delta^{18}\text{O}$ values for the thin layer tubes are lower than those of the mounds (-2.12 ‰ VPDB compared to -1.28 ‰ VPDB). Carbon and oxygen stable isotope values do not appear to co-vary within any of the three sample populations.

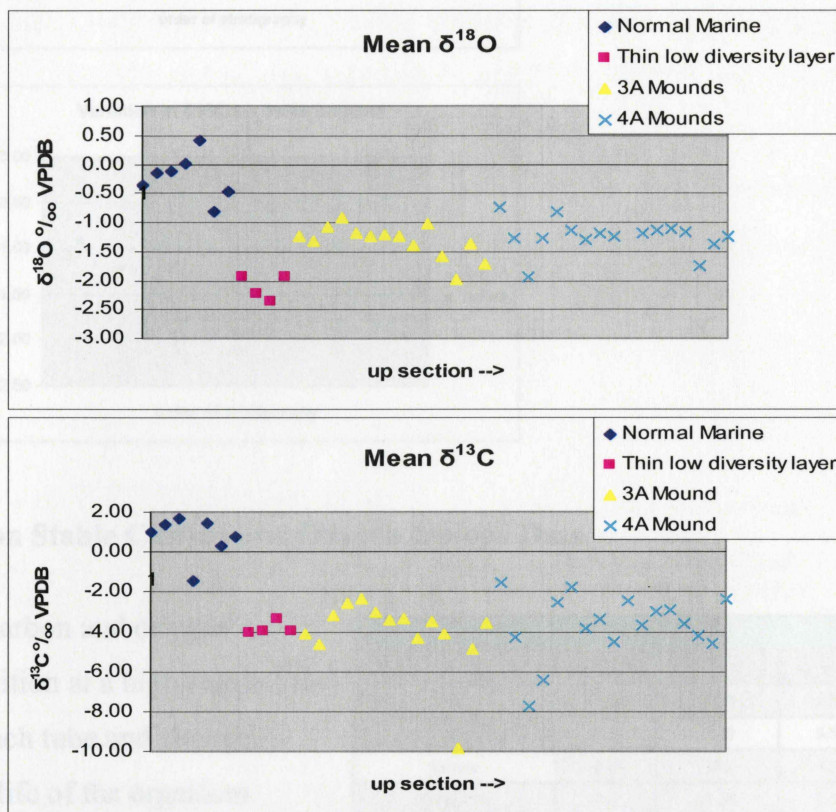


Figure 10a (above and below). Plots displaying the average $\delta^{13}\text{C}$ and $\delta^{18}\text{O}$ values of tubes from three areas of tube growth. Mound sample population is divided by tier number: tiers 3a and 4a are represented.

Figure 11 shows the average $\delta^{13}\text{C}$ and $\delta^{18}\text{O}$ values for the tier 3a/4a transect. It is apparent that tubes sampled from the contact between the third and fourth tiers vary widely in $\delta^{13}\text{C}$ and $\delta^{18}\text{O}$ values. Values of samples taken further away from the contact zone seem to fluctuate more regularly around a baseline average value in contrast to the erratic values of tubes found at the transition between tiers.

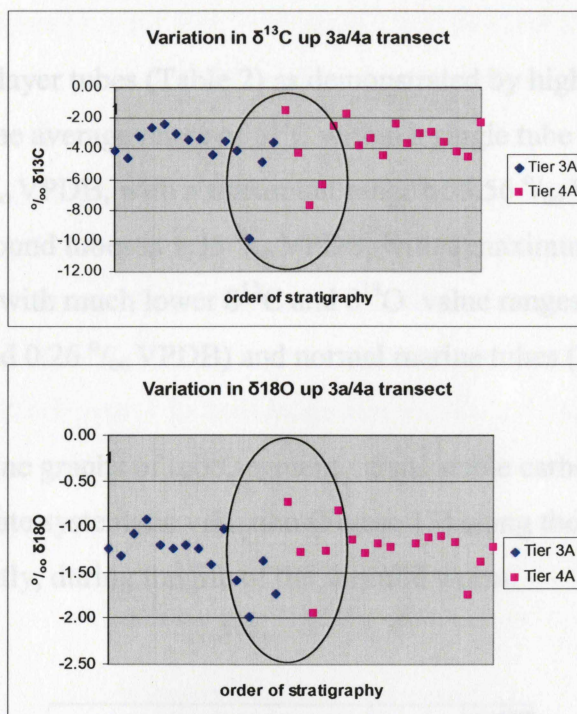


Figure 11. Plots displaying the average $\delta^{13}\text{C}$ and $\delta^{18}\text{O}$ values for tubes sampled along the tiers 3a/4a transect. Note highest variability exists among data points (within circle) at the contact between tiers.

High Resolution Stable Carbon and Oxygen Isotope Data

Stable carbon and oxygen isotope composition at a high resolution varies within each tube and changes throughout the life of the organism. Bulk data indicates that mound tubes exhibit the greatest variability in average $\delta^{13}\text{C}$ and $\delta^{18}\text{O}$ values throughout the period of mound formation, and high resolution data confirms this trend on a shorter timescale. The range of $\delta^{13}\text{C}$ and $\delta^{18}\text{O}$ during the life span of a single organism is greater for mound tubes than both normal marine and thin low

Table 2 (at right). Chart displaying statistical analysis of stable isotopic ratios. Mean and range are shown for a collection of 17 tubes from 3 different locales, totaling 105 samples.

MOUND TUBES				
Sample	Mean ^{13}C	Mean ^{18}O	Range ^{13}C	Range ^{18}O
4a12	-2.50	-1.25	2.33	.37
4a1	-7.47	-2.40	5.56	2.28
4aBase	-3.35	-.56	4.30	1.88
3aTopTier	-2.97	-1.54	4.09	.51
3aTop4	-5.96	-.93	1.99	.90
3aTop3	-2.97	-1.64	1.69	0.24
3aBTM10	-4.73	-.78	2.81	.75
3aBTM8	-3.69	-1.39	3.63	1.30
3aBTM5	-4.95	-1.14	4.94	3.76
3aBTM1	-3.64	-1.42	2.80	.76
LM	-2.35	-1.51	1.90	.41
Average 3a Tubes	-4.13	-1.26	3.13	1.18
Average 4a Tubes	-4.44	-1.40	4.06	1.51
TRIAL COLONIZATION TUBES				
Sample	Mean ^{13}C	Mean ^{18}O	Range ^{13}C	Range ^{18}O
209	-3.39	-2.41	1.29	.32
801	-3.96	.199	.38	.18
808	-4	-2.11	.96	.29
Average T.C. Tubes	-3.78	-.84	.88	.26
NORMAL MARINE TUBES				
Sample	Mean ^{13}C	Mean ^{18}O	Range ^{13}C	Range ^{18}O
216	1.02	-.35	2.07	.61
220	1.67	-.12	2.48	2.48
817	.74	-.47	2.27	2.66
Average N.M. Tubes	1.14	-.31	2.27	1.92

diversity layer tubes (Table 2) as demonstrated by high resolution sampling and analysis.

The average range of $\delta^{13}\text{C}$ within a single tube for the mound sample population is 3.60 ‰ VPDB, with a maximum range of 5.56 ‰ VPDB. The average range of $\delta^{18}\text{O}$ within mound tubes is 1.35 ‰ VPDB, with a maximum range of 3.76 ‰ VPDB. This contrasts with much lower $\delta^{13}\text{C}$ and $\delta^{18}\text{O}$ value ranges within thin layer tubes (0.88 ‰ VPDB and 0.26 ‰ VPDB) and normal marine tubes (2.27 ‰ VPDB and 1.92 ‰ VPDB).

Line graphs of tube segment versus stable carbon and oxygen isotope composition demonstrate systematic variation (Figure 13) along the length of each tube and, equivalently, during the life of the serpulid worm.

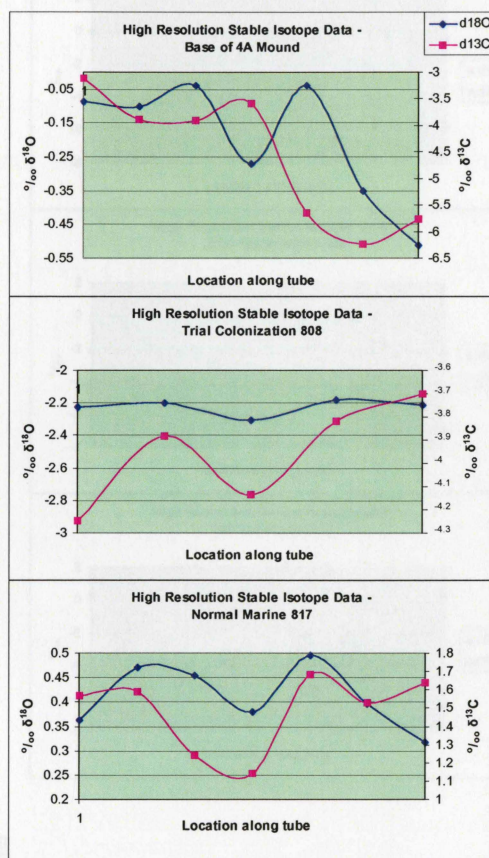


Figure 13. Line graphs of tube segment (progressing continuously) versus $\delta^{13}\text{C}$ and $\delta^{18}\text{O}$ values for three individual tubes. Plots are scaled according to ranges of $\delta^{13}\text{C}$ and $\delta^{18}\text{O}$ values for each tube in order to highlight oscillations – note each plot is scaled differently.

Although each plot in Figure 13 is scaled suitably to augment any systematic fluctuation in stable isotope values for individual tubes, closer examination reveals that the tier 4a tube exhibits the most variability in both $\delta^{13}\text{C}$ and $\delta^{18}\text{O}$. All tubes nonetheless show changes in $\delta^{13}\text{C}$ and $\delta^{18}\text{O}$ values at some scale.

Figure 14 compares plots of the results of high resolution sampling for the same three tubes represented in Figure 13. Instead of customizing the axes according to the ranges of $\delta^{13}\text{C}$ and $\delta^{18}\text{O}$ values, in Figure 13 each axis is scaled the same in order to illustrate the disparity in both range and mean stable carbon and oxygen isotope values for each tube. The tube that grew at the base of a tier 4a mound exhibits the most variability in both stable carbon and oxygen isotope values.

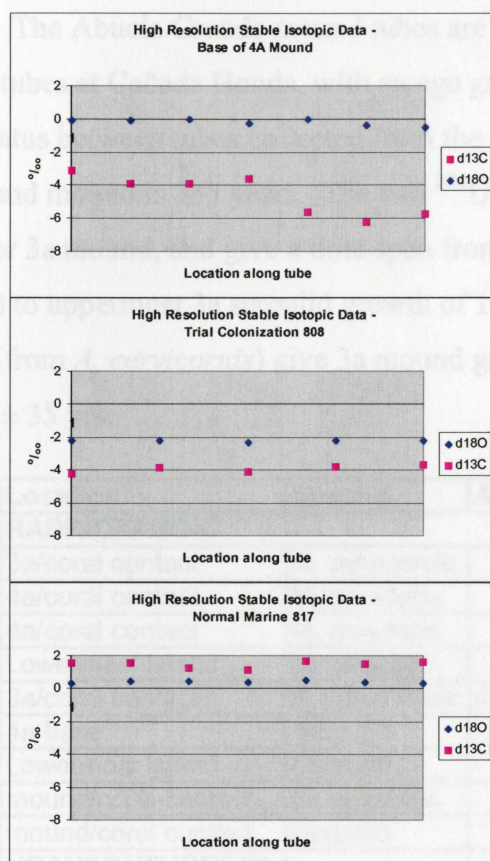


Figure 14. High resolution stable isotopic data of three serpulid tubes taken from a normal marine setting, the thin low diversity serpulid layer, and a fully developed mound. Plots are scaled the same (-4 to 2 per mil) in order to highlight differences in range and mean composition.

Age dating

Radiocarbon and $^{234}\text{U}/^{230}\text{Th}$ age dating results are given in Table 3. The youngest date comes from an island mound serpulid tube ($3860 \text{ ybp} \pm 35 \text{ yrs}$) and an Abuela

Grande mound tube (3700 ybp \pm 35 yrs). The oldest dated serpulid tubes were collected from 3a (6004 ybp \pm 119 yrs) and 4a (4205 ybp \pm 35 yrs) mounds.

The oldest coral, *A. cervicornis* underlying a 3a mound, was dated at 5420 ybp \pm 35 yrs. The youngest corals, *M. annularis* underlying island mounds, were dated at 4995 and 4990 ybp \pm 35 yrs. The range of coral dates is only 430 years. *M. annularis* from underneath the island mounds is younger (4990 ybp \pm 35 yrs) than *M. annularis* from the 4a contact (5195 ybp \pm 35 yrs). All of the coral age dates, including the youngest, are greater than all of the serpulid tube age dates, with the exception of the tube taken from the 3a/coral contact.

The time interval between colonizing serpulid tubes and coral substrate ranges from 990 to 1120 years at Cañada Honda (abbreviated CH) and 1275 years at Abuela Grande (AG). The Abuela Grande mound tubes are closest in age to the lowermost island mound tubes at Cañada Honda, with an age gap of 160 years.

The hiatus between tubes collected from the uppermost fourth tier and the lowermost island mound is 335 years. The two $^{234}\text{U}/^{230}\text{Th}$ age dates are from the top and bottom of a tier 3a mound, and give a time span from lowest 3a serpulid growth (6004 ybp \pm 119 yrs) to uppermost 3a serpulid growth of 1105 years. However, other 3a base contact dates (from *A. cervicornis*) give 3a mound growth lower age limits of 5420, 5040, and 4355 ybp \pm 35 yrs.

Location	Species	Age (Ka)	Locale
RADIOCARBON			
3a/coral contact	<i>A. cervicornis</i>	5420	CH
4a/coral contact	<i>M. annularis</i>	5195	CH
4a/coral contact	<i>M. annularis</i>	5185	CH
Lowermost Island	<i>M. annularis</i>	4990	CH
3a/coral contact	<i>A. cervicornis</i>	4355/5040	CH
4a base	Serpulid	4205	CH
Lowermost Island	Serpulid	3870	CH
mound/coral contact	<i>M. annularis</i>	4975	AG
mound/coral contact	Serpulid	3700	AG
URANIUM/THORIUM			
4a/3a contact	Serpulid	4899	CH
3a/coral contact	Serpulid	6004	CH

Table 3. Chart showing ages of radiocarbon and $^{234}\text{U}/^{230}\text{Th}$ dated samples. Both corals and serpulids were dated at several contacts to develop a time sequence of colonization.

Figure 15 (following page). Schematic diagram of Cañada Honda mound profile. Age dates of some mounds and coral substrates are given next to their illustration.

DISCUSSION

There are three distinct settings of mounds

morphology and age. Individual mounds grew around

and were thus presumably living in normal marine waters

there is a thin jet stratigraphically distinct micropaleontological

at 2000) that overlies reef deposits and indicates that

divergent settlement is therefore thought to represent

colony because separate accumulation is a

suggests a given longer lasting annularis colony

earlier

highly aggregated colony, the

not consistent with an

not to have flourished in some

of coral growth

with a change from a normal marine

is taken from the three settings support

found in the small colony are restricted

is mound and the reef colonization layer

levels of vertically dispersed light carbon

with a

and the mound is highly

depleted in $\delta^{13}C$ and $\delta^{15}N$

interact

able to get

while conducive to the

short-

of

fully

the

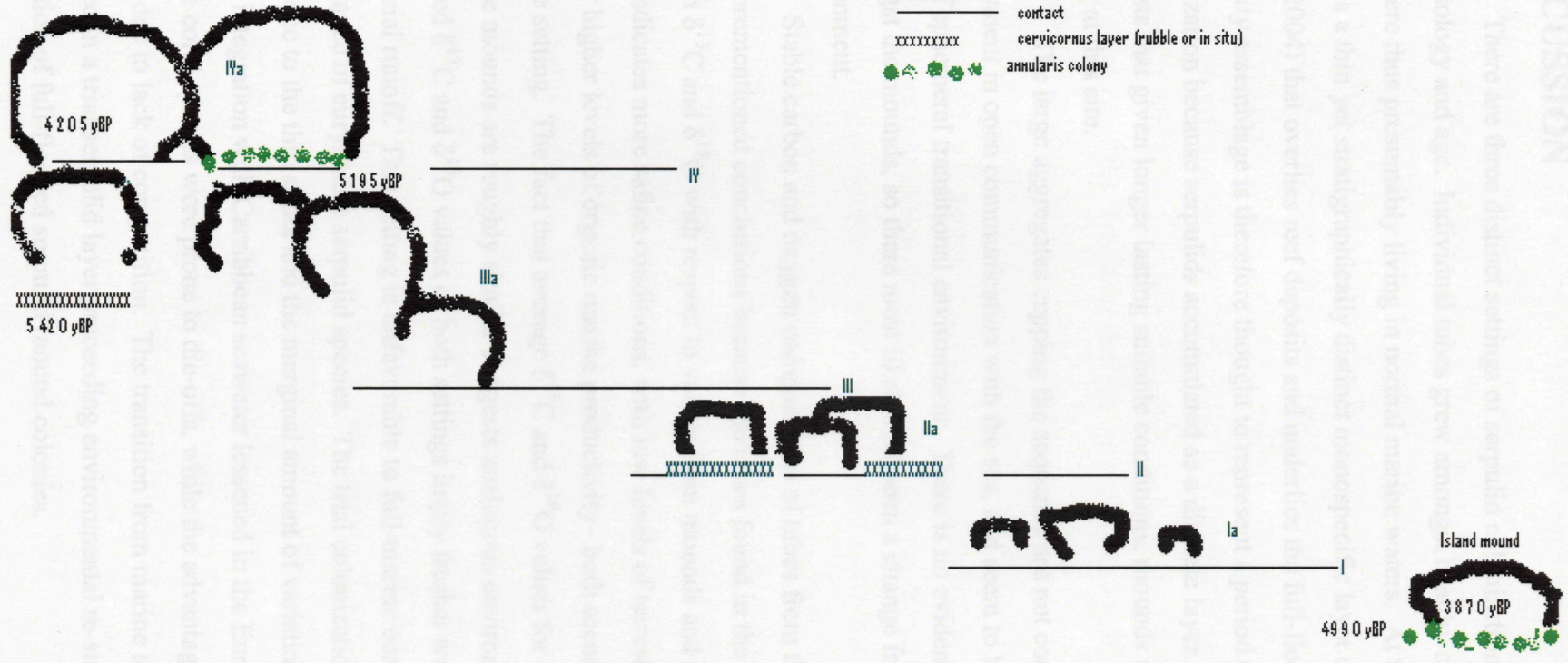
probably

the

and the

the

Explanation	
	mound
	contact
XXXXXXXXXX	cervicornus layer (rubble or in situ)
	annularis colony



DISCUSSION

There are three distinct settings of serpulid colonization, as distinguished by morphology and age. Individual tubes grew amongst healthy coral in the reefal facies, and were thus presumably living in normal marine waters. At the Abuela Grande locale, there is a thin yet stratigraphically distinct monospecific layer of serpulid tubes (Guerard et al, 2004) that overlies reef deposits and underlies the full-fledged mounds. This low diversity assemblage is therefore thought to represent a period of trial mound colonization because serpulids accumulated as a discrete layer. This morphology suggests that given longer lasting suitable conditions, mounds would have developed earlier at this site.

The large aggregates capping the sequence are not consistent with an embayment in open communication with the sea, and seem to have flourished in some sort of ephemeral transitional environment. There is no evidence of coral growth amongst the mounds, so there most likely had been a change from a normal marine environment.

Stable carbon and oxygen compositions of tubes from the three settings support the aforementioned conclusions because the tubes found in the reefal facies are enriched in both $\delta^{13}\text{C}$ and $\delta^{18}\text{O}$ with respect to values from mounds and the trial colonization layer. This indicates more saline conditions, with low levels of terrestrially derived light carbon and/or higher levels of organic marine productivity— both scenarios are consistent with a marine setting. The fact that average $\delta^{13}\text{C}$ and $\delta^{18}\text{O}$ values for the trial colonization layer and the mounds are roughly similar suggests analogous environments of formation. The depleted $\delta^{13}\text{C}$ and $\delta^{18}\text{O}$ values of both settings imply fresher water and higher levels of terrestrial runoff. This setting is unfavorable to full-marine corals while conducive to the dominance of euryhaline serpulid species. The trial colonization layer was likely short-lived, due to the thin strata and the marginal amount of variation in $\delta^{13}\text{C}$ and $\delta^{18}\text{O}$ values. When integration with Caribbean seawater lessened in the Enriquillo embayment, fully marine coral species were prone to die-offs, while the advantageous serpulids began to thrive due to lack of competition. The transition from marine to lacustrine probably resulted in a trial serpulid layer preceeding environmental re-stabilization and the formation of full-fledged serpulid mound colonies.

Given that both $\delta^{13}\text{C}$ and $\delta^{18}\text{O}$ values of the normal marine tubes are significantly higher than the other two locales (Figure 10), this sample suite likely formed in a normal marine environment. Low $\delta^{13}\text{C}$ and $\delta^{18}\text{O}$ values of the trial colonization tubes and mounds suggest warmer and/or low salinity water and potentially higher levels of terrestrial carbon, perhaps a result of increased runoff into the lake from a diversion into the lake of the Rio Georges (Greer and Swart, in press). This is consistent with a hyposaline scenario. As the embayment began to fill with alluvial sediment, Lago Enriqueillo became a giant "bowl," filling up with rainwater and terrestrial runoff. The water level would also have risen if the restriction occurred too quickly for evaporation rates to catch up. This allows for the formation of early serpulid mounds tens of meters above the current lake level.

Radiocarbon dates shed light on the order of formation of the different mound strata (Figure 15) and provide information on the nature of the contact between mound and coral. Samples from the lowermost mounds record the youngest age indicating formation during a regression. While elevation measurements for the sampled Abuela Grande mound were not taken, the age of this tube suggests coincident formation with the island mounds at Cañada Honda. The age dates of tubes and substrate, when applied to the mapped stratigraphic architecture, show a broadly regressive sequence; however, the mound terraces can't represent a strictly regressive scenario because tier 4a sits directly atop tier 3a. Dates indicate that tier 3a took as long as 1000 years to develop before some hiatus occurred and tier 4a was established. Interestingly, this time interval is much greater than the one separating tier 4a and the lowermost mounds. The small age difference between tier 4a and island mound suggests that despite elevation difference, the capping and lowermost mounds may have been developing at the same time, and/or that growth rates of the youngest mounds were rapid. This provides further evidence for the ephemeral nature of the embayment restriction and formation of Lago Enriqueillo, meaning freshwater input fluctuated and/or the seaway cut-off and reformed during a > 1000 year time period. This also points towards the ability of serpulids to colonize in variable settings and withstand rapid and/or dramatic environmental shifts.

Coral age dates reinforce the latter conclusion. *M. annularis* underlying serpulid mounds may have formed after the termination of the main reef and the formation of the

earliest mounds. These sporadic coral colonies represent the last gasp of marine life in between periods of significant terrestrial input and closing stages of Caribbean sea circulation. Traces of encrusting and boring species on the exterior of mounds may also signify a temporary return to marine conditions (higher salinity, less variability) after initial seaway cutoff. The greater than 1,000 yr hiatus between coral substrate termination and overlying mound growth indicates that serpulids were not developing on live coral. The transient nature of the restricted environment did not necessarily produce rapid facies changes – serpulid colonization took place well after the end of coral growth.

Results from high resolution sampling of serpulid tubes corroborate the idea that mound architecture stems from environmental fluctuations. Rather than purely mechanical sea level change, the differences between tiers may be attributed to substantial oscillations in water temperature, salinity, and/or terrestrial input. The fact that $\delta^{13}\text{C}$ values for the mounds yield the highest variability and are lowest of all three serpulid settings may be accounted for by periodic diversions of the Rio Yaque del Sur into the restricted embayment. The lagoonal mound environment might have experienced higher levels of terrestrial carbon due to runoff; a scenario consistent with fluctuations in fluvial contribution.

In addition, samples taken from the contact between the third and fourth tiers vary widely in stable carbon and oxygen isotope composition. This may be a sign of disequilibrium in the environment between the termination of tier 3a and the development of tier 4a, such as a period of storm intensification. The amount of variation displayed in $\delta^{18}\text{O}$ values at this mound transition is too dramatic to be accounted for by temperature changes alone and is likely the result of salinity changes brought about by even a single catastrophic storm. Observations of the effects of modern-day storms, such as Hurricane George in 1998 have shown that one large meteorological event can result in the temporary diversion of nearby rivers and a substantial salinity decrease. Overall, the wider range of mound $\delta^{13}\text{C}$ and $\delta^{18}\text{O}$ values as compared to the normal marine tubes denotes a highly variable environment. This geochemical signature verifies what is physically observed in the field – a distinct transition between mound tiers (see Methods, Figure 7.)

CONCLUSION

The data presented in this paper may show that mound formation reflects larger-scale climate trends. Throughout the Holocene, Caribbean climate trended towards warmer and wetter. Studies of other proxies from other regions provide conclusive evidence for this development. Using ostracods from Lake Miragoane, Haiti, Hodell et al (1991) demonstrate that both $\delta^{13}\text{C}$ and $\delta^{18}\text{O}$ ratios dip after the end of the last ice age signaling an end to cool and dry conditions, then stabilize at lower values implying a sustained warm/wet period beginning roughly 8000 ybp. The timing of the latter period coincides with the flooding of the Enriquillo embayment and the development of the fringing reef sequences; the oldest *A. cervicornis* specimens were dated at 9377 ybp. Heightened precipitation would have contributed to increased sedimentation at the mouth

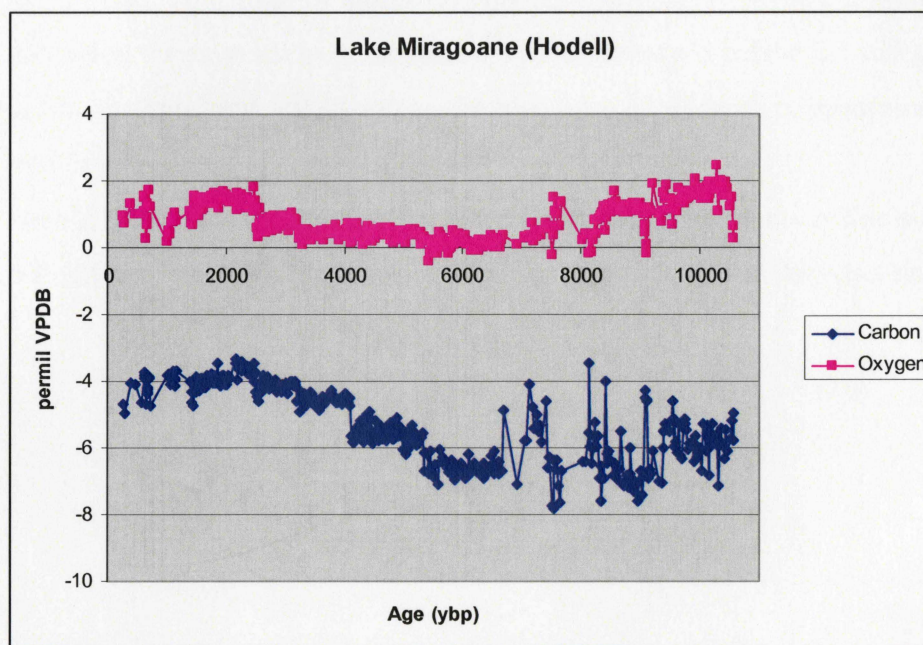


Figure 16 (above). Data from Hodell et al (1991) using ostracods as a proxy for Holocene climate change from 10,500 to 0 ybp.

of the bay, resulting in the eventual filling of the embayment mouth. The dates of the first mounds ($4899 \text{ ybp} \pm 75 \text{ yrs}$) occur within the warm/wet period, whereas the youngest mounds ($3700 \text{ ybp} \pm 35 \text{ yrs}$) date to the initial rise of $\delta^{13}\text{C}$ and $\delta^{18}\text{O}$ values (occurring at roughly 3000 ybp), signaling the beginning of more arid conditions. Therefore, the mounds represent the greater overall climate shift from warm and wet to

more arid, manifested locally by the restriction of normal marine circulation in the Enriquillo Valley and the establishment of a hyposaline, lagoonal environment. Mounds accumulated in a regressive sequence, likely following a receding shoreline as evaporation subjugated precipitation beginning approximately 3000 ybp.

It is important to continue studying these unusually large serpulid tube mounds because shifting regional climate patterns may have contributed to final restriction of the Enriquillo embayment and termination of coral reef growth. Hopefully understanding this small piece of the puzzle will contribute to greater overall insight into Holocene climate change for the wider Caribbean region.

Many thanks to Rick Mortlock and Rick Fairbanks at Lamont-Doherty Earth Observatory and Bill Patterson of University of Saskatchewan for teaching me to run my own samples. Also, Al Curran of Santa College and Neil Tibert of the University of Mary Washington for sage advice. Thanks as well to Kelsey Windsor for being a wonderful field partner, and Julie Jackson for two years of research collaboration, support, and laughter.

I would not have enjoyed the many hours spent studying in my office nearly so much had it not been for the very honest observations and coffee of Brendan Smith.

ACKNOWLEDGEMENTS

I owe the completion and success of this project to my advisor, Lisa Greer, who not only inspired my initial pursuit of geology but also continued to encourage and fuel my interest in earth science. I'm so appreciative of Lisa and the rest of the geology professors at Washington & Lee University for being such wonderful examples of how to combine a love of science and research while living full lives outside of school.

I am indebted to the R.E. Lee Summer Research Program, the W&L Geology department, and the Keck Geology Consortium for providing me with the opportunities to grow and learn through independent research.

Many thanks to Rick Mortlock and Rick Fairbanks at Lamont-Doherty Earth Observatory and Bill Patterson of University of Saskatchewan for teaching me to run my own samples. Also, Al Curran of Smith College and Neil Tibert of the University of Mary Washington for sage advice. Thanks as well to Kelsey Windsor for being a wonderful field partner, and Julie Jackson for two years of research collaboration, support, and laughter.

I would not have enjoyed the many hours spent studying in my office nearly so much had it not been for the very honest observations and coffee of Brendan Smith.

REFERENCES

- Andrews, P.B., 1964. Serpulid reefs, Baffin Bay, Southeast Texas. *Depositional Environments, South-Central Texas Coast: Field Trip Guidebook, October 30-31, Gulf Coast Association of Geological Societies, Annual Meeting in Corpus Christi*, p. 102-120.
- Behrens, E.W., 1968. Cyclic and current structures in a serpulid reef. *Contributions in Marine Science*, v. 13, p. 21-27.
- Glumac, B., Berrios, L., Greer, L., and Curran, H.A., 2004. Holocene tufa-coated serpulid mounds from the Dominican Republic: Depositional and diagenetic history, with comparison to modern serpulid aggregates from Baffin Bay, Texas. *Proceedings of the 11th Symposium on the Geology of the Bahamas and Other Carbonate Regions*: San Salvador, Gerace Research Center, p. 49-65.
- Greer, L. and Swart, P.K., *in review*, Decadal cyclicity of regional Mid-Holocene precipitation as driven by tropical Atlantic sea surface temperatures: Evidence from Dominican coral proxies. *Submitted to Paleoceanography*, 2005.
- Guerard, G.M.M., Greer, L., Curran, H.A., 2004. Environmental indicator proxies from a mid-Holocene coral reef, Enriquillo Valley, Dominican Republic. *Proceedings of the 11th Symposium on the Geology of the Bahamas and Other Carbonate Regions*: San Salvador, Gerace Research Center, p. 35-48.
- ten Hove, H.A. and van den Hurk, P., 1993. A review of Recent and fossil serpulid 'reefs'; actuopalaentology and the 'Upper Malm' serpulid limestones in NW Germany. *Geologie en Jijnbouw*, v. 72, p. 23-67.
- Jackson, J.E., 2005. High resolution dating and characterization of *Acropora Cervicornis* growth in the Enriquillo Valley, 9.45 – 6.06 KA (U/TH). *Geological Society of America Abstracts with Programs*, v. 37, No. 7, p. 364.
- Mann, P., Taylor, F.W., Burke, K., Kulstad, R., 1984. Subaerially exposed Holocene coral reef, Enriquillo Valley, Dominican Republic. *Geological Society of America Bulletin*, v. 95, p. 1084-1092.
- Mortlock, R.A., Fairbanks, R.G., Chiu, T., Rubenstone, J., 2005. $^{230}\text{Th}/^{234}\text{U}/^{238}\text{U}$ and $^{231}\text{Pa}/^{235}\text{U}$ age from a Single Fossil Coral Fragment by Multi-collector Magnetic-sector Inductively Coupled Plasma Mass Spectrometry. *Geochimica et Cosmochimica Acta* v.69, p. 649-657.
- Schubert, A., 2000. El Lago Enriquillo – Patrimonio Natural y Cultural del Caribe. *Published in Santo Domingo, Republica Dominicana by Presidencia de la Republica, Direccion Nacional de Parque, Rep. Dom.* 50 p.
- Taylor, F.W., Mann, P., Valastro, S., Jr., and Burke, K., 1985. Stratigraphy and radio-carbon chronology of a subaerially exposed Holocene coral reef, Dominican Republic: *Journal of Geology*, v. 93, p. 311-332.

APPENDIX A: HIGH RESOLUTION DATA

Sample ID	$\delta^{13}\text{C}$	$\delta^{18}\text{O}$	
842-A	0.333	1.437	
842-B	0.371	1.568	location
842-C	0.383	1.531	
842-D	0.466	1.468	
842-E	0.476	1.313	along
842-G	0.425	1.383	
842-H	0.368	1.68	
842-I	0.402	1.397	tube
842-J	0.344	1.482	
842-K	0.352	1.55	
842-L	0.369	1.596	
842-M	0.387	1.531	
842-N	0.459	1.613	
842-O	0.289	1.492	
842-P	0.447	1.316	
842-Q	0.708	1.567	
842-R	0.526	1.467	
842-S	0.648	1.492	
2162-A	-0.026	1.599	
2162-B	-0.146	1.076	
2162-D	-0.371	1.569	
2162-E	-0.548	1.343	
2162-F	-0.635	-0.475	
808AB	-1.751	-4.229	
808D	-2.02	-3.409	
808E	-2.04	-4.371	
808	-2.223	-4.246	
	-2.2	-3.882	
	-2.303	-4.133	
	-2.18	-3.819	
	-2.213	-3.702	
309	-0.289	-1.859	
	0.157	-1.448	
	0.194	-1.098	
209	-2.475	-3.083	
	-2.158	-3.077	
	-2.45	-3.043	
	-2.402	-4.331	
801	-1.844	-3.715	
	-2.019	-4.085	
	-1.853	-4.098	

I7-18	-1.995	-3.862
34	-1.756	-3.312
I7-20	-1.837	-3.84
I7-21	-1.644	-4.587
I7-22	-1.925	-3.659
216	0.01	0.701
C7-26	-0.049	1.106
C7-27	-0.229	2.157
C7-28	-0.334	1.571
817	0.363	1.571
C7-30	0.471	1.593
C7-31	0.455	1.245
C4-1	0.381	1.144
C4-2	0.495	1.685
C4-3	0.396	1.527
C4-4	0.318	1.638
E4-1	-2.67	-1.38
E4-2	-2.14	-1.52
E4-3	-1.98	-1.59
E4-4	-2.73	-1.60
E4-5	-1.58	-1.71
E4-6	-2.13	-1.52
E4-7	-2.09	-1.47
E4-8	-3.48	-1.30
E4-9	-3.03	-1.61
E4-10	-2.75	-1.61
I7-1	-	-
C4-29	4.29758	1.50789
I7-2	-4.376	-1.724
I7-4	-	-
C4-30	4.44599	1.75012
I7-6	-	-
C4-31	4.64143	1.63674
I7-7	-	-
C4-32	3.98203	1.79377
I7-8	-2.702	-1.45
I7-9	-	-
C4-33	0.55427	1.28013
I7-10	-1.979	-1.915
I7-11	-1.349	-1.485
I7-12	-3.105	-0.085
I7-13	-3.894	-0.1
I7-14	-3.917	-0.039
I7-15	-3.582	-0.272
I7-16	-5.65	-0.038
I7-17	-6.23	-0.352

I7-18	-5.771	-0.512
I7-19	-3.422	-0.925
I7-20	-4.466	-1.098
I7-21	-3.782	-1.035
I7-22	-2.33	-0.752
I7-23	-2.843	-1.07
C7-26	-1.924	-1.82
C7-27	-1.707	-1.61
C7-28	-2.335	-2.24
C7-29	-4.033	-3.93
C7-30	-2.627	-2.53
C7-31	-3.852	-3.75
C4-1	-5.424	-5.32
C4-2	-2.653	-2.55
C4-3	-2.673	-2.57
C4-4/5	-5.388	-5.29
C4-6/7	-4.255	-4.16
C4-8/9	-4.782	-4.68
C4-10	-4.167	-4.07
C4-11	-3.511	-3.41
C4-12	-3.23	-3.13
C4-13	-6.391	-6.29
C4-14	-5.676	-5.58
C4-15	-6.762	-6.66
C4-16	-7.608	-7.51
C4-17	-6.759	-6.66
C4-18	-6.01	-5.91
C4-	-5.376	-5.28
19/20		
C4-21	-6.306	-6.21
C4-22	-4.766	-4.67
C4-	-1.778	-1.68
25/26		
C4-27	-4.071	-3.97
C4-28	-3.629	-3.53
C4-29	-5.409	-5.31
C4-31	-3.579	-3.48
C4-32	-4.838	-4.74
C4-33	-5.265	-5.17
C4-	-8.265	-8.17
35/36		
C4-37	-10.402	-2.752
C4-38	-8.589	-2.989
C4-39	-9.378	-1.854
C4-40	-8.746	-2.546

RESOLUTION DATA

mean 0180 range 0130 range 0180

-1.79	1.28	0.28
-1.91	1.90	0.41 v
-1.42	2.00	0.75 p
-1.14	4.94	3.76
-1.30	3.03	1.30 s
-0.78	2.01	0.75 a
-1.44	1.00	0.24 a
-0.02	1.90	0.90 i
-1.34	4.05	0.61 i
-0.50	4.30	1.88 a
-1.25	2.33	0.37 n
0.28	2.07	0.81
0.16	1.40	0.34
0.12	0.00	0.19
0.02	0.79	0.40
0.47	0.64	0.16
-0.07	3.07	2.30
0.42	2.27	2.05
1.34	0.06	0.29
2.02	0.54	3.12
-0.37	1.24	0.32
-1.93	0.38	0.16

COMPILED HIGH RESOLUTION DATA

Sample ID	mean $\delta^{13}\text{C}$	mean $\delta^{18}\text{O}$	range $\delta^{13}\text{C}$	range $\delta^{18}\text{O}$
MOUNDS				
34 (4)	-3.85	-1.79	1.28	0.28
Lowermost (10)	-2.35	-1.51	1.90	0.41 u
3aBtm1 (4)	-3.64	-1.42	2.80	0.76 p
3aBtm5 (11)	-4.95	-1.14	4.94	3.76
3aBtm8 (5)	-3.69	-1.39	3.63	1.30 s
3aBtm10 (5)	-4.73	-0.78	2.81	0.75 e
3aTop3 (5)	-2.97	-1.64	1.69	0.24 c
3aTop4 (4)	-5.96	-0.93	1.99	0.90 t
3aTopTier (4)	-2.97	-1.54	4.09	0.51 i
4aBase (7)	-3.35	-0.56	4.30	1.88 o
4a12 (6)	-2.50	-1.25	2.33	0.37 n
NORMAL MARINE				
216 (5)	1.02	-0.35	2.07	0.61
216 (4)	1.38	-0.15	1.46	0.34
220 (3)	1.67	-0.12	0.90	0.19
309 (3)	-1.47	0.02	0.76	0.48
817 (7)	1.49	0.41	0.54	0.18
817 (4)	0.31	-0.81	2.07	2.90
817 (7)	0.74	-0.47	2.27	2.66
TRIAL COLONIZATION				
808 (3)	-4.00	-1.94	0.96	0.29
808 (5)	-3.96	-2.22	0.54	0.12
209 (4)	-3.38	-2.37	1.29	0.32
801 (4)	-3.94	-1.93	0.38	0.18

APPENDIX B: BULK DATA

Sample ID	$\delta^{13}\text{C}$	$\delta^{18}\text{O}$	
B1	-4.13	-1.24	u
B2	-4.61	-1.32	p
B3	-3.16	-1.08	
B4	-2.61	-0.91	s
B5	-2.39	-1.20	e
B6	-3.04	-1.24	c
B7	-3.39	-1.20	t
B8	-3.34	-1.24	i
B9	-4.35	-1.40	o
B10	-3.49	-1.03	n
B15	-4.13	-1.59	
T3	-9.84	-1.98	
T4	-4.88	-1.37	
T7	-3.56	-1.73	
4A 0	-1.49	-0.74	
4A 1	-4.31	-1.28	
4A 2	-7.68	-1.94	
4A 3	-6.39	-1.26	
4A 4	-2.51	-0.83	
4A 5	-1.72	-1.14	
4A 6	-3.80	-1.29	
4A 7	-3.34	-1.19	
4A 8	-4.47	-1.23	
4A 9	-2.40	outlier	
4A 10	-3.62	-1.18	
4A 11	-3.00	-1.12	
4A 12	-2.92	-1.11	
4A 15	-3.57	-1.17	